On Strength Functions for Orthotropic Brittle Materials

C. L. Huang*
Kansas State University, Manhattan, Kansas

BASED upon the strength-tensor theory proposed by Gol'denblat, et al.,[1] Huang[2,3] determined the second, fourth, and sixth rank strength-tensors in the three-dimensional case for each of the crystal classes, from consideration of invariant transformations of the strength function. The invariants for a strength function having orthotropic symmetry are then used to determine, explicitly, the cubic form of the strength function for orthotropic media.[4] The main purpose of the present paper is to formulate a strength function for orthotropic brittle materials which takes both the Bauschinger effect and the influence of stress interaction into account. Also, for simplicity, only the components of the second and fourth strength tensors for orthotropic brittle media are considered. The components of the strength tensors are expressed in terms of engineering strengths, which are determined directly from tests of the orthotropic brittle materials. To demonstrate the method of application, the strength functions for Graph-I-Tite-Grade G[5] and Grade ATJ[6] are presented as examples.

For the class of orthotropic symmetry, the numbers of linearly independent stress invariants of the first and second are three and nine, respectively. The strength function is then expressed as a quadratic form[3,4]

$$F(\sigma_i) = (F_1\sigma_1 + F_2\sigma_2 + F_3\sigma_3)^{\alpha} + (F_{11}\sigma_1^2 + F_{22}\sigma_2^2 + F_{33}\sigma_3^2 + 2F_{12}\sigma_1\sigma_2 + 2F_{23}\sigma_2\sigma_3 + 2F_{13}\sigma_1\sigma_3 + F_{44}\sigma_4^2 + F_{55}\sigma_5^2 + F_{66}\sigma_6^2)^{\beta} - 1 = 0 \quad (1)$$

The axes of elastic symmetry of orthotropy are designated as coordinate axes, (x_1,x_2,x_3). By taking $\alpha=\beta=1$ in Eq. (1), the quadratic form of the strength function can be expressed as the matrix form

$$F_i\sigma_i + F_{ij}\sigma_i\sigma_j = 1 \quad (2)$$

in which

$$F_i = \begin{bmatrix} F_1 \\ F_2 \\ F_3 \\ 0 \\ 0 \\ 0 \end{bmatrix}, \quad F_{ij} = \begin{bmatrix} F_{11} & F_{12} & F_{13} & 0 & 0 & 0 \\ F_{12} & F_{22} & F_{23} & 0 & 0 & 0 \\ F_{13} & F_{23} & F_{33} & 0 & 0 & 0 \\ 0 & 0 & 0 & F_{44} & 0 & 0 \\ 0 & 0 & 0 & 0 & F_{55} & 0 \\ 0 & 0 & 0 & 0 & 0 & F_{66} \end{bmatrix}$$

By introducing the following symbols defined by Hill[8]

$$F=-F_{13}\ , \quad G=-F_{23}\ , \quad H=-F_{12}$$

$$2L=F_{44}\ , \quad 2M=F_{55}\ , \quad \text{and} \quad 2N=F_{66}$$

and by imposing the assumption of incompressibility, i.e.,

$$F_{11}=G+H\ , \quad F_{22}=H+F\ , \quad \text{and} \quad F_{33}=F+G$$

Equation (1) is reduced to the Hoffman criterion for orthotropic brittle media[7];

$$F_1\sigma_1 + F_2\sigma_2 + F_3\sigma_3 + F(\sigma_2-\sigma_3)^2 + G(\sigma_3-\sigma_1)^2 + H(\sigma_1-\sigma_2)^2 + 2L\sigma_4^2 + 2M\sigma_5^2 + 2N\sigma^2 = 1 \quad (3)$$

Furthermore, if the absence of Bauschinger effects is assumed, the second order strength tensor F_i vanishes, and Eq. (3) yields to the Hill criterion for anisotropic media[8]

$$F(\sigma_2-\sigma_3)^2 + G(\sigma_3-\sigma_1)^2 + H(\sigma_1-\sigma_2)^2 + 2L\sigma_4^2 + 2M\sigma_5^2 + 2N\sigma_6^2 = 1 \quad (4)$$

The twelve strength components $F_1,\ldots,F_{66}$ in Eq. (2) are intrinsic material parameters, and must be determined experimentally from the basic engineering strengths of an orthotropic medium. The results are[3]

$$F_1 = \frac{1}{X_t} - \frac{1}{X_c}, \quad F_2 = \frac{1}{Y_t} - \frac{1}{Y_c}, \quad F_3 = \frac{1}{Z_t} - \frac{1}{Z_c},$$

$$F_{11} = \frac{1}{X_tX_c}, \quad F_{22} = \frac{1}{Y_tY_c}, \quad F_{33} = \frac{1}{Z_tZ_c}$$

$$F_{13} = -\tfrac{1}{2}\left[\frac{1}{R_t^{(45^\circ)}R_c^{(45^\circ)}} - \frac{1}{Z_tZ_c} - \frac{1}{X_tX_c}\right]$$

$$F_{23} = -\tfrac{1}{2}\left[\frac{1}{Q_t^{(45^\circ)}Q_c^{(45^\circ)}} - \frac{1}{Y_tY_c} - \frac{1}{Z_tZ_c}\right]$$

$$F_{12} = -\tfrac{1}{2}\left[\frac{1}{S_t^{(45^\circ)}S_c^{(45^\circ)}} - \frac{1}{X_tX_c} - \frac{1}{Y_tY_c}\right]$$

$$F_{44} = \frac{1}{Q^2}, \quad F_{55} = \frac{1}{R^2}, \quad F_{66} = \frac{1}{S^2} \quad (5)$$

where

(X_t,Y_t,Z_t) = Tensile strengths in (x_1,x_2,x_3) directions, respectively.

(X_c,Y_c,Z_c) = Compressive strengths in (x_1,x_2,x_3) directions, respectively.

(S,R,Q) = Shearing strengths in the planes of symmetry $(x_1x_2,x_1x_3),x_3x_2)$ in the directions of the axes of symmetry, respectively.

Presented as Paper 75-1008 at the AIAA Aircraft Systems and Technology Meeting, Los Angeles, Calif., Aug. 4-7, 1973; submitted August 22, 1975; revision received December 1, 1975. The author expresses his sincere thanks to R. E. Ely and T. L. Weng for their generosity in providing the test data.

Index category: Materials, Properties of.

*Professor, Department of Mechanical Engineering. Member AIAA.

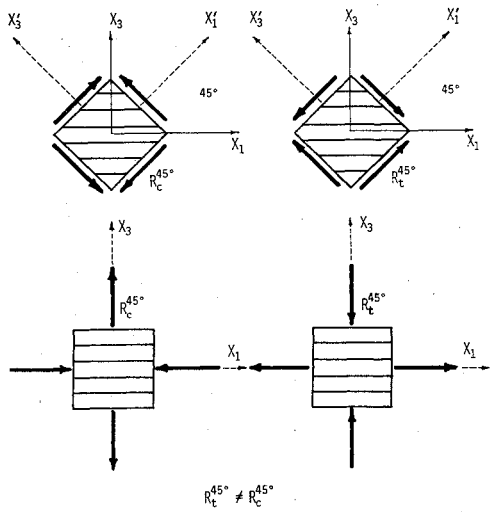

Fig. 1 The shear strengths in the symmetric plane z_1x_3 along the directions x_1' and x_3'—axis.

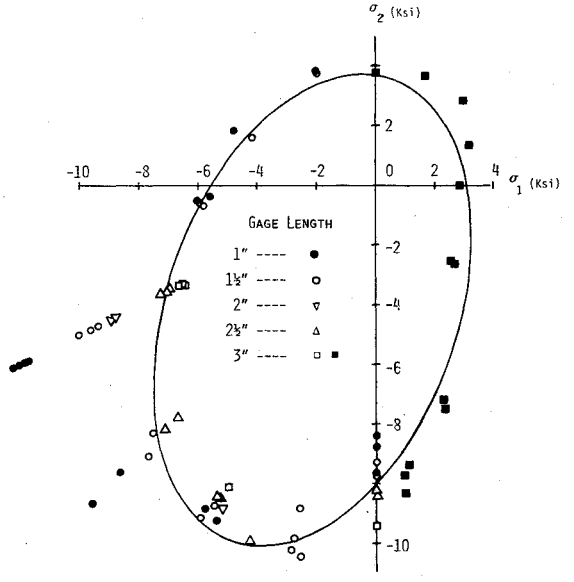

Fig. 2 Strength function for graph - 1- tite.

$(S_t^{(45°)}, R_t^{(45°)}, Q_t^{(45°)})$ = Position shearing strengths in the planes of symmetry (x_1x_2, x_1x_3, x_3x_2) along with the new coordinates (x_1^*, x_2^*), (x_1', x_2'), ($x_3^\ddagger, x_3^\ddagger$), respectively. See Fig. 1.

$(S_c^{(45°)}, R_c^{(45°)}, Q_c^{(45°)})$ = Negative shearing strengths in the planes of symmetry (x_1x_2, x_1x_3, x_2x_3), along with the new coordinates (x_1, x_2), (x_1', x_3'),($x_3^\ddagger, x_3^\ddagger$) respectively. See Fig. 1.

Table 1 Engineering strengths of Graph-I-Tite, a high density polycrystalline graphite

x_t	=3,100 psi	x_c	= 5,500 psi
Y_t	=3,700 psi	Y_c	=10,000 psi
$S_t^{(45°)}$	=2,900 psi	$S_c^{(45°)}$	= 3,100 psi*

Table 2 Engineering strengths for Grade ATJ Graphite

x_t	=3,500 psi	x_c	= 6,800 psi
Y_t	=2,700 psi	Y_c	=10,000 psi
$S_t^{(45°)}$	=3,400 psi	$S_c^{(45°)}$	= 3,000 psi

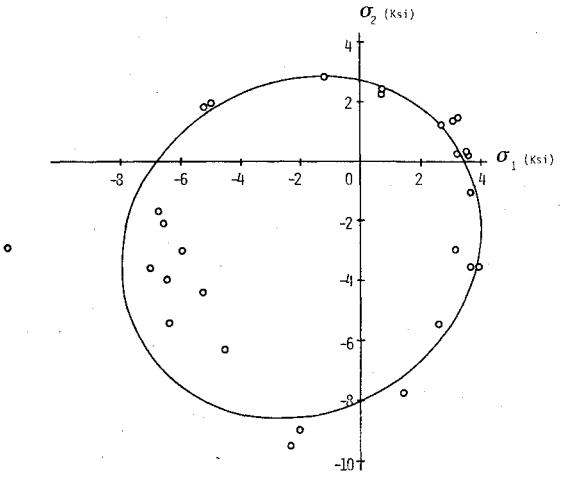

Fig. 3 Strength function for grade ATJ graphite.

While the triaxial fracture stresses for orthotropic brittle materials are practically non-existent, the most extensive experimental results of biaxial fracture stresses for Graph—I-Title-Grade G[5] and Grade ATJ Graphite,[6] available to the writer, are used for the verification of the proposed criterion. The experimental results are obtained by three test methods: (1) short-tube method, (2) long-tube method, and (3) pressure-vessel method (See Refs. 5 and 6). Results are summarized in Tables 1 and 2 were the strength data $S_c^{(45°)}$ is obtained by the method of interpolation.

The components of strength tensors F_i and F_{ij} can be calculated from Eq. (5) with the engineering strengths given above. The results are: a) Graph-I-Tite: $F_1 = 1.4076 \times 10^{-4}$, $F_2 = 1.7027 \times 10^{-4}$, $F_{11} = 5.8651 \times 10^{-8}$, $F_{22} = 2.7027 \times 10^{-8}$, and $F_{12} = -1.2778 \times 10^{-8}$.

b) Grade ATJ Graph: $F_1 = 1.3866 \times 10^{-4}$, $F_2 = 2.4537 \times 10^{-4}$, $F_{11} = 4.2017 \times 10^{-8}$, $F_{22} = 4.6296 \times 10^{-8}$, $F_{12} = 0.4863 \times 10^{-8}$.

The strength functions for Graph-I-Tite and Grade ATJ Graphite with zero shearing stress σ_6 are plotted in Fig. 2 and Fig. 3, where the experiment data were obtained by Ely and Weng, respectively.

Figures 2 and 3 show that the agreement between the proposed criterion and the experimental results is good except in the compression-compression ($c-c$) biaxial-stress quadrant. for those tests $c-c$ stress quadrant, the fracture modes are dominated by the geometric parameters of tubular specimens, such as the thickness-diameter ratio and the thickness-length ratio. In other words, the instability and the arch-action of the tubular specimens have a significant influence on the strength in the $c-c$ stress quadrant. This partly explains the reason for a wide scatter in strength data of the orthotropic brittle material. For other types of test specimen, the strength of the materials might be different from those strengths obtained by the tubular specimen test. Thus, it is suggested that additional experimental work on strength with other types of specimens is needed in $c-c$ stress quadrant.

Finally, it is worthy to note that the present proposed strength function is a simple failure criterion, which takes the Bauschinger effect and stress interaction into account. The components of strength tensors F_i and F_{ij} satisfy the invariant property. Also Hoffman's and Hill's criteria are the special cases of this general criterion proposed.

References

[1] Gol'denblat, I. I. and V. A. Kopnov, "Strength of Glass-Reinforced Plastics in the Complex Stress State," *Mekhanika Polimerov*, Vol. 1, 1965, p. 70.

[2] Huang, C. L., "On Quadratic Strength Function for Anisotropic Materials," *Proceedings of the 1974 Symposium on Mechanical Behavior of Materials*, Kyoto, Japan, 1974.

[3]Huang, C. L., "On Strength Function for Anisotropic Materials," *Proceedings of Symmetry, Similarity and Group-Theoretic Methods in Mechanics*, The University of Calgary, Canada, 1974.

[4]Huang, C. L. and Kirmser, P. G., "A Criterion on Strength for Orthotropic Materials," *Fiber Science and Technology*, 1975, to be published.

[5]Ely, R. E., "Strength Results for Two Brittle Materials Under Biaxial Stresses," U. S. Army Missile Command—Redstone Arsenal Alabama, Technical Rept. RR-72-11, 1972.

[6]Weng, T. L., "Grade ATJ Graphite," *Proceedings of the Conference on Continuum Aspects of Graphite Design*, Nov. 9-12, Gatlinburg, Tennessee, CONF-701105, NTIS, U.S. Dept. of Commerce, 1970.

[7]Hoffman, O., "The Brittle Strength of Orthotropic Materials," *Journal of Composite Materials*, Vol. 1, 1967, pp. 200-206.

[8]Hill, R., "A Theory of the Yielding and Plastic Flow of Anisotropic Metals," Procedings Royal Society (London), A, 193, 1948, pp. 281-297.

Calculation of Compressible Turbulent Boundary Layers on Straight-Tapered Swept Wings

P. Bradshaw*
Imperial College, London, England
G. A. Mizner†
Queen Mary College, London, England
and
K. Unsworth‡
Imperial College, London, England

Introduction

THE turbulent boundary layer on a constant-chord swept wing (or infinite yawed wing) is aerodynamically three-dimensional, because the velocity and shear-stress vectors do not coincide in plan view; but it is computationally two-dimensional, because derivatives along the generators are zero.[1-4] Infinite yawed wings are a useful approximation to real wings, but it does not seem to have been realized that calculations for straight-tapered wings (a very good approximation to many real wings) are only slightly more complicated. Here we describe the extension of an infinite-wing program to the case of a straight-tapered wing. The program calculates compressible flow with or without heat transfer.

Over the outer, straight-tapered part of the wing shown in Fig. 1, derivatives of external-flow quantities along the generators (spanwise) are nearly zero except near the tip. Because the boundary-layer thickness varies along the generators, spanwise derivatives within the boundary layer are not zero, but they can easily be related to derivatives normal to the surface, so that, as on an infinite yawed wing, calculations are needed at only one spanwise station, from which results at other stations follow by scaling with the local chord. The full equations for nonaxisymmetric flow in cylindrical polar coordinates are given by Rodi:[5] his x, r, θ correspond to the present y, r_0-z, x/r_0, respectively. All equations contain extra terms which can be loosely described as rotation-of-axes terms. The Reynolds-stress transport equations contain extra generation terms which are individually of the same order as the rotation-of-axes terms but whose net effect is much smaller. Nash and Scruggs[6] used a cylindrical polar coordinate system in calculations of the turbulent boundary layer on the straight-tapered wing shown in Fig. 1; they neglected the extra generation terms without explanation, and did not notice that derivatives along the generators could be simplified.

Received September 17, 1975. This work was supported by Ministry of Defence (PE) under contract AT/2037/0133: helpful discussions with the project monitor, L. F. East, are gratefully acknowledged.

Index category: Boundary Layers and Convective Heat Transfer—Turbulent.

*Reader in Fluid Dynamics.
†Research Student.
‡Postdoctoral Research Assistant.

Table 1 Calculations of Nash and Scruggs[6] for the swept wing of Fig. 1 at $M_\infty = 0.5$. C_F = chordwise-average skin-friction coefficient

Station	A	B	C	D	E
$10^3\delta^*_{TE}/c$	2.49	2.75	2.71	2.72	3.62
$10^3 C_F$	3.40	3.50	3.54	3.62	3.62

Nash's and Scruggs' predictions of the skin friction coefficient, and of the displacement thickness divided by local chord at the trailing edge of the wing shown in Fig. 1 are given in Table 1. The variation along the span is negligible, as our straight-taper approximation would predict, except near the crank and the tip; a small Reynolds-number effect on skin friction can be seen. The report from which Nash and Scruggs took the pressure distributions is not publicly available so we have not been able to check the present method against their calculations (which used a slightly simplified version of the present turbulence model). However their finding that the isobars on a real straight-tapered wing conicide quite closely with the generators, even at $M_\infty = 0.99$, justifies the approach in the present paper.

The Program

We have programed the compressible heat transfer version[7] of the boundary-layer calculation method of Bradshaw and Ferriss,[8] for straight-tapered wings. The extension of the incompressible isothermal version to infinite swept wings was described in Ref. 2 and the present version is essentially the same aerodynamically. The two components of the Reynolds shear stress τ, $-\overline{\rho u v}$ and $-\overline{\rho v w}$, are predicted by transport equations, which are a logical extension to three dimensions of the empirical shear stress transport equation derived from the turbulent energy equation in Ref. 8. It should be noted that this shear-stress equation is conceptually equivalent to those derived by later workers from the exact shear-stress transport equation; it has the advantage of being based on an exact equation whose main terms have been measured. The heat-transfer calculation uses a slightly refined version of the usual assumption of constant Prandtl number. In contrast to integral methods, crossover profiles present no difficulty. The main advantage over the integral methods actually available for three-dimensional flows is the use of a modern turbulence

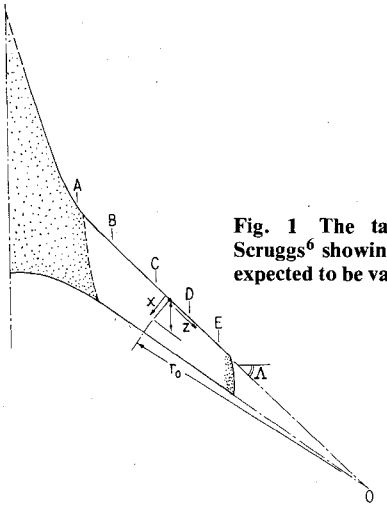

Fig. 1 The tapered wing of Nash and Scruggs[6] showing the present axes. Method is expected to be valid outside dotted regions.